Correcting π-delocalization errors in conformational energies using density-corrected DFT, with application to crystal polymorphs

Bhaskar Rana,[1*] Gregory J. O. Beran,[2] and John M. Herbert[1†]
[1] *Department of Chemistry and Biochemistry, The Ohio State University, Columbus, Ohio 43210 USA*
[2] *Department of Chemistry, University of California, Riverside, California 92521 USA*
(Dated: September 26, 2022)

Abstract

We consider several molecules characterized by π-electron conjugation whose extent changes along a flexible torsional coordinate, and which represent the monomer units of polymorphic molecular crystals. Delocalization error in density functional theory (DFT) adversely impacts conformational energies in these species, overstabilizing the conformation that maximizes conjugation length and leading to incorrect relative energies for the corresponding crystal polymorphs. We demonstrate that density-corrected (DC-)DFT, in which a DFT exchange-correlation functional is evaluated using a Hartree-Fock density, significantly reduces these conformational energy errors. When DC-DFT monomer energies are used as a low-cost intramolecular correction to a periodic DFT calculation of the molecular crystal, the resulting relative polymorph energies are within 1 kJ/mol of benchmark results.

I. Introduction

Crystal packing plays an important but difficult-to-predict role in controlling physical properties of organic molecular crystals, including solubility, shelf stability, and bioavailability.[1–3] Polymorphism,[1–4] or the potential to form multiple distinct crystal packing motifs, is critically important to the pharmaceutical industry,[3,5] as highlighted by the case of the HIV drug ritonavir, where the appearance of a previously-unknown and low-solubility polymorph made it impossible to produce the original polymorph and forced a drug recall.[6] Other pharmaceutical examples of such "disappearing polymorphs" are known,[7–9] and more recently it has been suggested that the thermodynamically stable crystal form has not been found experimentally for 15–45% small-molecule drugs currently available on the market.[10]

Over the past decade, *ab initio* crystal structure prediction has moved from the category of "impossible", as it was famously characterized 30 years ago,[11,12] to merely "extremely challenging".[13–23] Successful crystal structure prediction, including quantitative ranking of low-energy polymorphs, is most feasible for small-molecule species with limited conformational flexibility.[24–26] Quantitative prediction of thermodynamically stable polymorphs comes with stringent accuracy requirements, as an estimated 50% of polymorph pairs differ by less than 2 kJ/mol and around 95% of the conformers differ by less than 8 kJ/mol.[4,27,28]

Dispersion-corrected density functional theory (DFT+D) had made enormous strides towards making crystal structures predictable from first principles,[22,29–34] but this success is mitigated in certain cases by overstabilization of delocalized π-electron systems,[26,28,35,36] which is a consequence of self-interaction error (SIE).[37] This issue is thought to impact polymorph prediction in well-known examples such as the anti-cancer drug axitnib,[26] the organic semiconductor molecule rubrene,[38] the well-studied ROY molecule,[26,28,35,39,40] molecule X[26,41] from the third blind test of crystal structure prediction,[42] as well as other systems.[26,36,43] Structures for several of these molecules are shown in Fig. 1. Each of these molecules exhibits conformational polymorphism whereby changes in intramolecular conformation access different intermolecular crystal packing motifs. Notably, in each of these molecules the extent of π-electron delocalization changes as a function of one or more intramolecular torsional coordinates. To the extent that delocalization error may overstabilize the more highly-conjugated conformations, we expect that DFT will produce erroneous conformational energy profiles for these flexible monomers. Those errors propagate into errors in the relative energies for the crystal polymorphs formed from these monomers.[26,28,35,39] Given the small energy differences between polymorphs, even modest conformational energy errors can have a qualitative impact on polymorph stability ordering.

In principle, these issues can be addressed using more advanced electronic structure models, but application of such methods to periodic crystals of pharmaceutical-sized molecules is generally cost-prohibitive. A more pragmatic approach combines a conventional periodic DFT calculation using a generalized gradient approximation (GGA) with an intramolecular correction based on the difference between the baseline DFT functional and a more advanced model, computed for a gas-phase molecule.[26] For example, using the B86bPBE+XDM functional,[44–46] a GGA that includes a dispersion correction based on the exchange dipole moment (XDM),[46] in combination with dispersion-corrected second-order

*Present address: Dept. of Chemistry, Stanford University, Stanford, CA 94305 USA
†herbert@chemistry.ohio-state.edu

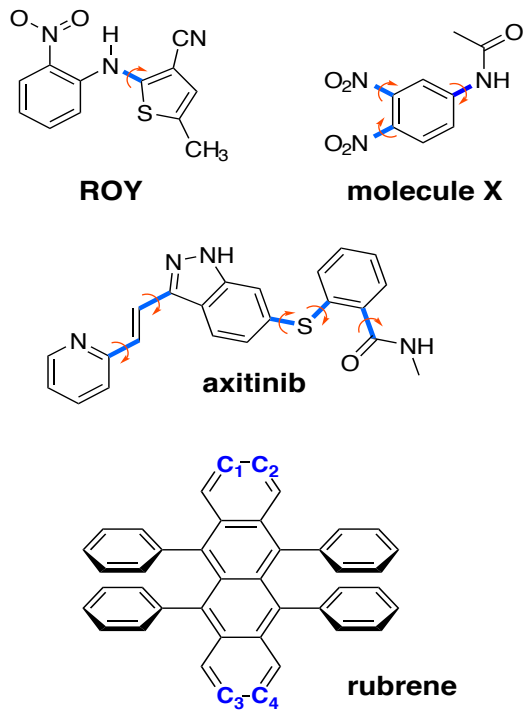

Figure 1: Structures of the four molecules investigated in this work, indicating the torsional angles that modify the conjugation length. In rubrene, it is a twisting of the C_1–C_2–C_4–C_3 dihedral angle that modulates the conjugation.

Møller-Plesset perturbation theory (MP2D),[47,48] the resulting polymorph stability rankings are consistent with experiment for ROY, acetamidobenzamide, and axitinib.[26,40]

A possible alternative solution to the π-delocalization problem comes in the form of density-corrected (DC-)DFT.[49–55] In this approach, an approximate density functional $\tilde{E}[\rho]$ is evaluated using a density ρ_{HF} that is obtained at the Hartree-Fock (HF) level:

$$E_{\text{DC-DFT}} = \tilde{E}[\rho_{\mathrm{HF}}] \,. \tag{1}$$

This procedure, which has also been called HF-DFT,[56,57] has been shown to correct some of the worst delocalization problems associated with GGA functionals, including those with reaction barrier heights,[57–59] torsional barriers,[60] halogen bonding,[61] potential energy surfaces for main-group radicals,[49–51] and polaron defects in metal oxide materials.[59] In the present work, we investigate the ability of DC-DFT to correct conformation energies of the π-delocalized systems in Fig. 1, and examine how that impacts the predicted stabilities of the corresponding polymorphs.

II. Methods

A. DC-DFT

In conventional Kohn-Sham DFT, the approximate energy functional $\tilde{E}[\rho]$ is minimized with respect to ρ. The resulting energy approximates what would be obtained via optimization of an exact functional $E[\rho]$, if the latter were known. Burke, Sim, and coworkers[49–55] suggest that it is pedagogically useful to separate the error $\tilde{E} - E$ into two contributions: a functional-driven part

$$\Delta E_{\mathrm{F}} = \tilde{E}_{\mathrm{xc}}[\rho] - E_{\mathrm{xc}}[\rho_0] \tag{2}$$

that originates in the approximate nature of the exchange-correlation (XC) functional, and a density-driven error

$$\Delta E_{\mathrm{D}} = \tilde{E}[\tilde{\rho}] - \tilde{E}[\rho_0] \,. \tag{3}$$

Here, $\tilde{\rho}$ indicates the density obtained by variational minimization of $\tilde{E}$, as in an ordinary self-consistent DFT calculation, whereas ρ_0 indicates the exact ground-state density obtained upon minimization of the exact functional $E[\rho]$. For cases where $|\Delta E_{\mathrm{D}}| \gg |\Delta E_{\mathrm{F}}|$, the overall error may be reduced by evaluating the approximate functional using a SIE-free density (such as ρ_{HF}) rather than a self-consistent one.[49,52–55]

With this idea in mind, the DC-DFT energy functional in Eq. (1) can be written more explicitly as

$$E_{\text{DC-DFT}}[\rho] = \tilde{E}\Big[\arg\min_{\rho}\left(E^{\mathrm{HF}}[\rho]\right)\Big] \,. \tag{4}$$

This form makes it clear that ρ_{HF} must first be obtained from a self-consistent HF calculation, starting from the input density ρ. Following this, the energy is obtained by evaluating the approximate functional $\tilde{E}[\rho]$ using the density ρ_{HF}. A more detailed expression for the same DC-DFT energy is

$$E_{\text{DC-DFT}}[\rho] = E^{\mathrm{HF}}[\rho] + \left(\tilde{E}_{\mathrm{xc}}[\rho_{\mathrm{HF}}] - E_{\mathrm{x}}^{\mathrm{HF}}[\rho]\right) \,, \tag{5}$$

where $E^{\mathrm{HF}}[\rho]$ is the HF total energy functional whereas $E_{\mathrm{x}}^{\mathrm{HF}}[\rho]$ is its exchange component, and $\tilde{E}_{\mathrm{xc}}[\rho]$ is the XC part of $\tilde{E}[\rho]$. The expression in Eq. (5) recognizes that the functionals $E^{\mathrm{HF}}[\rho]$ and $\tilde{E}[\rho]$ differ only in their XC parts, whereas the kinetic energy, Hartree self-repulsion, and nuclear–electron (or "external") potential terms are the same.

The DC-DFT procedure sacrifices self-consistency, which implies that the functional defined in Eqs. (4) and (5) is not variational. This necessitates modification to the analytic gradient.[57,59] Lack of self-consistency also means that DC-DFT is not beneficial in all cases,[55,62] but rather only cases that are dominated by density-driven error. Delocalization driven by SIE tends to fall into the category of density-driven error, as evident from the fact that DC-DFT based on GGA functionals significantly improves results for radicals[49–51,59] and barrier

heights.[57–59] (Transition states are usually characterized by partially-broken bonds and thus fractional charges on different chemical moieties, a classic SIE problem.[63,64])

A "density sensitivity" metric (S) has been suggested to determine whether a given problem is dominated by ΔE_{F} or ΔE_{D}.[53–55] This metric is defined as

$$S = \left|\tilde{E}[\rho_{\mathrm{LDA}}] - \tilde{E}[\rho_{\mathrm{HF}}]\right| \tag{6}$$

for an approximate functional $\tilde{E}[\rho]$, where ρ_{HF} is the self-consistent HF density and ρ_{LDA} is the self-consistent density computed using the local density approximation (LDA). Burke and co-workers[54,55] suggest $S > 2$ kcal/mol as an indicator of cases that are likely to be dominated by density-driven error (or $S > 8$ kJ/mol in the units that will be used herein), although that threshold was calibrated using small molecules. For larger systems with unpaired spins, one can find examples where S ranges from 150–650 kJ/mol across a set of similar chemical systems.[59] This suggests using

$$S_{\mathrm{atom}} = S/N_{\mathrm{atoms}} \tag{7}$$

as a metric that is normalized for system size.[59]

B. Monomer-Corrected DFT

In this work, DC-DFT and other models will be used to correct intramolecular conformational energies and then the monomer correction approach[26] is employed to examine the impact of the corrected conformational energies on polymorph stabilities. In this approach, one first performs a periodic DFT calculation on the full crystal, and herein that energy ($E^{\mathrm{DFT}}_{\mathrm{crystal}}$) is computed using the B86bPBE+XDM functional, as in previous work.[26,40] Then, for each of the N molecules in the unit cell, one computes a gas-phase energy difference between the low-level DFT treatment that is used for the periodic calculation ($E^{\mathrm{DFT}}_{\mathrm{molec},i}$) and a more advanced level of theory ($E^{\mathrm{high}}_{\mathrm{molec},i}$), where the "high-level" method could be DC-DFT or else a correlated wave function method. The crystal energy approximated in this way is

$$E_{\mathrm{crystal}} = E^{\mathrm{DFT}}_{\mathrm{crystal}} + \sum_{i=1}^{N}\left(E^{\mathrm{high}}_{\mathrm{molec},i} - E^{\mathrm{DFT}}_{\mathrm{molec},i}\right) . \tag{8}$$

In the present work, the high-level method will be computed with SIE-free model, whereas B86bPBE+XDM is responsible for modeling the intermolecular interactions. The summation in Eq. (8) can usually be simplified by exploiting symmetry equivalences of molecules within the unit cell. The geometries used for the gas-phase molecular corrections are those extracted directly from the crystal structure.

C. Computational Details

All the DC-DFT calculations were performed using the Q-Chem software.[65] For consistency with previous work, DFT-optimized crystal structures for axitinib, ROY, and molecule X, along with their intramolecular conformations, were taken directly from Ref. 26. B86bPBE+XDM crystal energies and gas-phase monomer calculations for use in Eq. (8) were also taken from Ref. 26. All other gas-phase DFT single-point energy calculations were performed using the aug-cc-pVQZ basis set and the SG-2 integration grid.[66] We use the D3 dispersion correction[67] with BeckeJohnson damping, DFT+D3(BJ). Density sensitivities S in Eq. (6) were evaluated using the SCAN functional[68] for $\tilde{E}[\rho]$, with aug-cc-pVQZ basis set.

Additional calculations using the spin-component scaled (SCS-)MP2D method[48] are provided for comparison with the DFT results. SCS-MP2D subtracts out the uncoupled HF dispersion[69] from MP2, replacing it with coupled Kohn-Sham dispersion.[70] Finally, spin components of the MP2 correlation energy are empirically scaled.[48] This approach is inspired by Heßelmann's corrected MP2 (MP2C) model,[71] the key difference being that the SCS-MP2D correction is framed in terms of the atom–atom D3 dispersion correction,[67] rather than intermolecular perturbation theory response functions. This makes SCS-MP2D applicable to both inter- and intramolecular interactions. SCS-MP2D does not suffer from SIE, and benchmark calculations demonstrate very good performance for challenging conformational energies.[48] SCS-MP2D results reported here were extrapolated to the complete basis set (CBS) limit based on calculations using aug-cc-pVTZ and aug-cc-pVQZ, following the procedure described in Ref. 26.

Relaxed conformational energy scans are examined for several of the molecules in Fig. 1, using geometries taken from the literature.[28,38] For the ROY molecule, the ∠S–C–N–C torsional angle indicated in Fig. 1 is used, whereas for rubrene and fluorinated derivatives thereof, the dihedral angle ∠C_1–C_2–C_3–C_4 was used. Single-point potential energy profiles here were then computed at the SCAN+D3, SCAN0+D3, and SCS-MP2D/CBS levels of theory. For ROY, the DFT calculations use the aug-cc-pVQZ basis set as indicated above, although for rubrene and its derivatives, aug-cc-pVTZ is used instead.

These results are compared to benchmarks obtained at the level of coupled-cluster theory with single, double, and perturbative triple excitations [CCSD(T)]. The benchmark results were taken from various sources. For molecule X, ROY, and rubrene, the CCSD(T)/CBS benchmarks were taken from Refs. 26, 28, and 38, respectively. For axitinib, CCSD(T)/CBS results were computed here at the domain-localized pair natural orbital (DLPNO-)CCSD(T_1) level,[72] using Orca v. 5.0[73] The latter benchmarks combined MP2/CBS results with a DLPNO-CCSD(T_1)/aug-cc-pVDZ correction, obtained using tight PNO settings and with `TCutMKN` $= 10^{-4}$.

Table 1: Density sensitivities [Eqs. (6) and (7)] for the molecules considered in this work.[a]

Molecule	Sensitivity (kJ/mol)	
	S	S_{atom}
ROY[b]	126.9 ± 2.2	4.70 ± 0.08
Molecule X[b]	153.0 ± 1.0	5.88 ± 0.04
Axitinib[b]	137.6 ± 1.4	2.99 ± 0.03
Rubrene[c]	123.9 ± 0.8	1.77 ± 0.01
Half-fluoro rubrene[c]	323.9 ± 1.2	4.63 ± 0.02
Perfluororubrene[c]	528.2 ± 1.2	7.55 ± 0.02

[a] Average across all conformers; uncertainties represent one standard deviation.
[b] Computed at the SCAN/aug-cc-pVQZ level.
[c] Computed at the SCAN/aug-cc-pVTZ level.

III. Results and Discussion

A. Density Sensitivities

Before analyzing energy landscapes for the molecules in Fig. 1, we first scrutinize the degree of density-driven error in these systems, as it has been observed that DC-DFT offers a better solution than conventional (self-consistent) DFT only when the density-driven error is large.[49,52–55] (Systems with significant static correlation also do not benefit from DC-DFT,[62] which is consistent with the idea that SIE may sometimes masquerade as strong correlation.[74]) We use the metric S in Eq. (6), evaluated using the SCAN functional, to assess density sensitivity. Based on small-molecule results, $S > 8$ kJ/mol has been suggested as a threshold beyond which DC-DFT is likely to improve the results.[54,55]

Table 1 provides values of S for various molecules considered in this work, computed as an average over all conformers since the variations from one conformer to the next are $\lesssim 2$ kJ/mol. (Differences in S from one conformer to the next will be considered later.) We obtain values ranging from $S = 124$–528 kJ/mol although our molecules are considerably larger than the ones used to set 8 kJ/mol as the threshold value. It has also been suggested that that S is not a size-extensive metric until the system is large enough for delocalization to attenuate naturally.[59] (In an infinite conjugated polymer described by a GGA functional, it is not clear that the delocalization length must ever terminate, as has been demonstrated for excitons described by time-dependent DFT with semilocal functionals.[75–77]) For the molecules considered here, the size-normalized metric S_{atom} [Eq. (7)] is as large as 7.6 kJ/mol. We will see that all of these molecules are affected by π-delocalization error, thus the 8 kJ/mol threshold (even if applied to S_{atom}) does not appear to be a sufficient diagnostic.

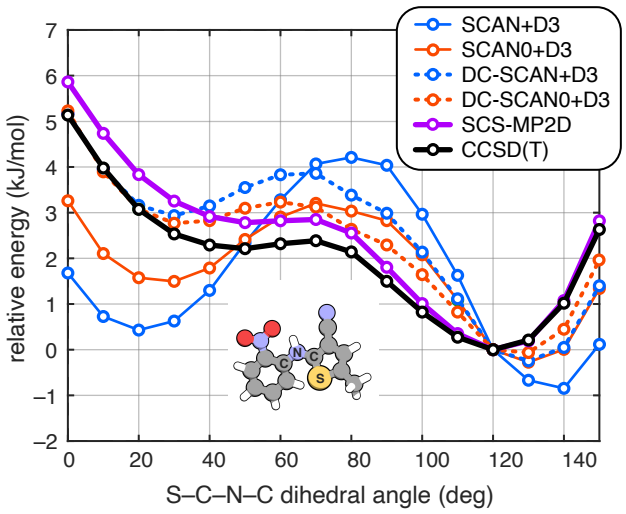

Figure 2: Relaxed potential energy scans of the ROY molecule along the ∠(S–C–N–C) dihedral angle (as indicated in the inset molecular structure), computed using the SCAN+D3 and SCAN0+D3 functionals their DC-DFT analogues. SCS-MP2D and the CCSD(T) benchmarks are also shown. Energy profiles are computed relative to the structure with a 120° dihedral angle, which is the minimum at the CCSD(T) level.

B. Torsional Energy Profiles

We next consider one-dimensional energy landscapes along some of the torsion angles suggested in Fig. 1. For the ROY molecule, intramolecular conformations found in its crystal polymorphs differ primarily by a single dihedral angle that is indicated in Fig. 2.[35,40,78–80] Dihedral angles between ≈ 50–$130°$ disrupt the π conjugation between the two aromatic rings, leading to a larger band gap and polymorphs that are yellow in color ("Y-"). More planar conformations increase the extent of π delocalization and shift the color towards red (polymorphs named "R-") or orange ("O-").

Previous work has shown that commonly-used GGA and hybrid functionals overstabilize the red and orange polymorphs relative to the yellow ones.[26,28,35,39,40,79] This can be understood as an SIE effect stemming from over-delocalization of the π electrons in near-planar geometries, where the system is better conjugated. As shown in Fig. 2, both GGAs and hybrid functionals over-stabilize the more planar conformations relative to benchmark CCSD(T) calculations. Hybrid functionals reduce the SIE and improve the conformational energy profile, but errors remain significant and are large enough to erroneously alter the polymorph stability rankings.[35,39] Torsional profiles computed using (DC-)B3LYP+D3 and (DC-)PBE0+D3 are shown in Fig. S1 and are similar to the (DC-)SCAN0+D3 results in Fig. 2.

Figure 3 plots torsional energy profiles of rubrene and some fluorinated derivatives thereof, along the

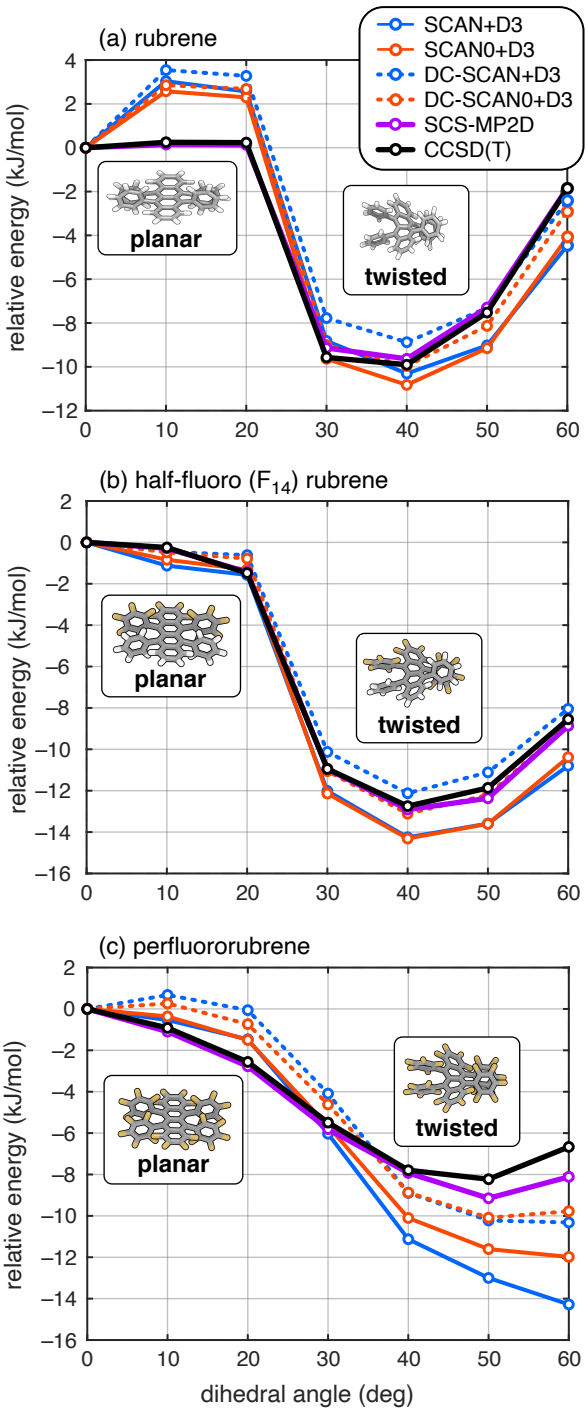

Figure 3: Relaxed one-dimensional scans of the (a) rubrene, (b) half-fluorinated (F_{14}) rubrene, and (c) perfluororubrene, along the dihedral coordinate $\angle C_1$–C_2–C_3–C_4 that is suggested in Fig. 1. The (DC-)DFT energies are computed using the aug-cc-pVTZ basis set. SCS-MP2D and CCSD(T) calculations are taken from from Ref. 38, and all structures are taken from that work as well.

$\angle C_1$–C_2–C_3–C_4 angle that is indicated in Fig. 1. (The fluorinated derivatives have been suggested as a means of tuning the noncovalent interactions and therefore the crystal structure,[81–83] modulating the band gap,[82,83] or to enhance stability with respect to oxidation.[84]) We refer to "planar" versus "twisted" configurations in Fig. 3 with respect to the core tetracene unit. As noted in previous work,[38] twist angles $\gtrsim 30°$ can increase conjugation, by bringing the π electrons of the aromatic side chains into play, and common density functionals thus overstabilize twisted orientations relative to planar ones, even while the twisted configuration is more stable according to CCSD(T) calculations.[38] In the case of the SCAN+D3 functional, DC-DFT improves the relative conformational energies of the planar (0°) and fully-twisted (60°) structures by 2–4 kJ/mol, although the twisted conformation is still somewhat overstabilized even with DC-DFT. This remains the case for the B3LYP+D3 and PBE0+D3 functionals also; see Fig. S2. With the SCAN0+D3 functional, DC-DFT improves the relative energies of the fully-twisted structures, and these energies match quite well with the CCSD(T) benchmark for the two out of three derivatives; see Figs. 3(a) and 3(b).

C. Relative Conformer and Polymorph Energies

The remainder of this work focuses on relative energies of ROY, molecule X, and axitinib, both as isolated molecules (considering the conformations found in the relevant crystal polymorphs) and in the crystalline phase, where the lattice energies are estimated using the monomer-correction scheme in Eq. (8).

The energy ordering of some ROY conformers are shown in Fig. 4(a), as computed using various density functionals (both self-consistent and DC-DFT) as well as SCS-MP2D and CCSD(T). According to CCSD(T) calculations,[26] the correct gas-phase conformational energy ordering is

$$\begin{aligned} \mathrm{YT04} < \mathrm{Y} < \mathrm{YN} < \mathrm{R} \approx \mathrm{OP} \approx \mathrm{ON} \\ < \mathrm{PO13} < \mathrm{ORP} < \mathrm{R05a} \approx \mathrm{R05b}\,. \end{aligned} \tag{9}$$

R05a and R05b refer to the two symmetry-unique molecular conformations found in the R05 polymorph. In the self-consistent DFT calculations, shown in the left panel of Fig. 4(a), all the dispersion-corrected GGA and meta-GGA functionals perform very poorly, over-stabilizing the red and orange conformers over the yellow ones by several kJ/mol. This can be understood as a SIE artifact, as discussed above. PBE+D3 shows the worst performance, completely reversing the energetic ordering relative to CCSD(T). Hybrid functionals partially mitigate the effect of SIE and behave better than the GGA functionals, and the hybrid meta-GGA functional SCAN0+D3 emerges as the best performer amongst the set of functionals tested here, although it still does not reproduce the CCSD(T) energy ordering.

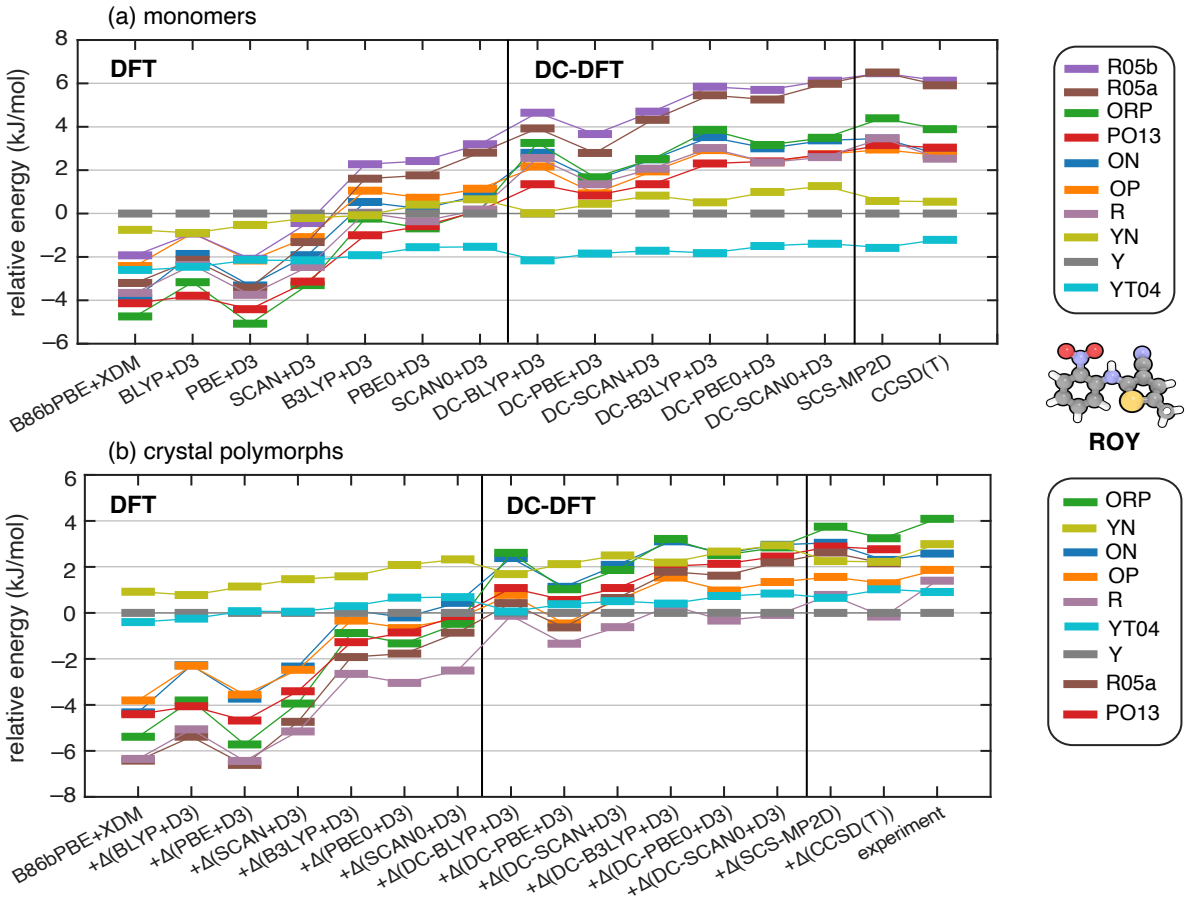

Figure 4: Energetic ordering of conformers of ROY (Fig. 1), computed using both self-consistent DFT and DC-DFT for the same set of functionals: (a) isolated monomer energies, and (b) crystal polymorph energies, computed using the monomer-correction scheme of Eq. (8). Energies are plotted relative to that of the Y conformer.

DC-DFT results for ROY are shown in the middle section of Fig. 4, for the same set of functionals. The DC procedure improves upon the self-consistent DFT results in all cases, coming much closer to the correct energetic ordering except in a few quasi-degenerate cases. This validates the hypothesis that π-delocalization error drives the erratic and mostly erroneous results obtained using conventional DFT. Lowest- and highest energy conformers are correctly predicted by DC-DFT for all functionals tested here, and the three lowest-energy conformers are correctly predicted by all of the DC-DFT methods except for DC-PBE+D3. Failure of the latter approach may be a sign of larger functional-driven error as compared to the hybrid functionals to the SCAN meta-GGA functional. Even for PBE+D3, however, the DC procedure moves the results closer to the correct energetic ordering as compared to the corresponding self-consistent DFT calculation. The DC-SCAN0+D3 and DC-PBE0+D3 methods afford correct energetic ordering for the most of the conformers, as judged by comparison to CCSD(T) benchmarks. The success of DC-SCAN and DC-SCAN0 has been noted in unrelated work.[85]

Having identified SCAN+D3 and SCAN0+D3 as the best of the self-consistent DFT approaches for the ROY molecule, let us return to the one-dimensional potential energy scans in Fig. 2. Both DC-SCAN+D3 and DC-SCAN0+D3 perform well in comparison to benchmark CCSD(T) calculations from Ref. 26, although neither is quite as faithful to the benchmark as is SCS-MP2D. In contrast, the self-consistent SCAN+D3 and SCAN0+D3 calculations yield erroneously large rotational barriers around 40–90°, as structures with angles of 0–30° are over-stabilized due to the SIE. Torsional energy profiles computed using (DC-)B3LYP+D3 and (DC-)PBE0+D3 are shown in Fig. S1 and exhibit most of the same trends that are seen for the hybrid (DC-)SCAN0+D3 level of theory in Fig. 2. Thus, the good performance of DC-SCAN+D3 and DC-SCAN0+D3 is not simply a matter of choosing a good functional to correct; the correction itself improves the results substantially.

Density sensitivities for ROY conformers are plotted in Fig. 5(a), computed using SCAN for the approximate functional $\tilde{E}[\rho]$ in Eq. (6). Yellow conformers (indicated by names starting with Y) exhibit smaller values of S

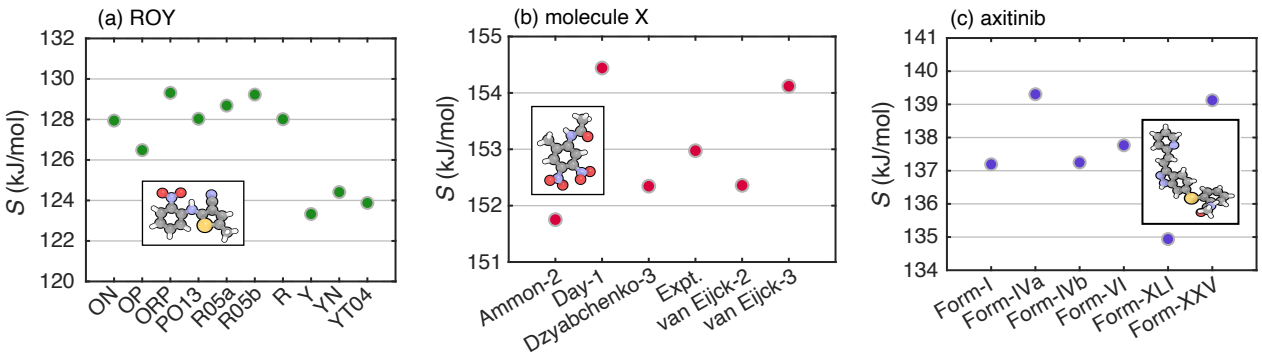

Figure 5: Density sensitivities [Eq. (6)] for different conformers of (a) ROY, (b) molecule X, and (c) axitinib, computed using SCAN/aug-cc-pVQZ for the approximate functional $\tilde{E}[\rho]$.

as compared to the other conformers, by $\approx$ 4 kJ/mol, a significant amount given the rather small energy differences between the various conformers. Larger SIE in near-planar geometries associated with the orange and red conformers explains the larger values of S in those cases. Application of DC-DFT thus selectively modifies the energy landscape of the conformers with the largest density sensitivity, meaning red and orange more so than yellow in this case. The result is a potential energy surface that pushes the energetic ordering in the right direction.

Up to this point we have discussed the behavior of an isolated molecule of ROY. Figure 4(b) reports the relative energies of the crystal polymorphs, computed using the monomer-correction scheme in Eq. (8) using various levels of theory. As reported previously,[26] the B86bPBE+XDM functional yields extremely poor relative energies with form Y, which is the thermodynamically most stable form, predicted to be the second-least stable polymorph. The relative order of the other lattice energies is also poor at this level of theory, relative to experimental lattice enthalpies or CCSD(T) lattice energies. Furthermore, replacing B86bPBE+XDM with another self-consistent GGA or hybrid functional does not meaningfully improve the energy rankings. In contrast, the DC-DFT models all perform much better. The close energy spacings of the ROY polymorphs make this a challenging problem for any method, but SCS-MP2D and DC-DFT with hybrid functionals all give fairly consistent qualitative rankings, even if the quantitative lattice energies differ.

We next perform a similar analysis for molecule X. The relevant conformers involve rotation of the bonds indicated with arrows in Fig. 1 and alter the extent of π conjugation with the central aromatic ring. According to CCSD(T) calculations,[26] the gas-phase energetic ordering of the various conformers is

$$\begin{aligned} &\text{van Eijck-3} < \text{van Eijck-2} < \text{Dzyabchenko-3} \\ &\quad < \text{Ammon-2} < \text{Expt.} < \text{Day-1}\ . \end{aligned} \tag{10}$$

The nomenclature in Eq. (10) reflects structures submitted by different groups in the third blind test of crystal structure prediction,[42] with "Expt." indicating the conformer in the experimental crystal structure. DFT calculations were previously found to reverse the order of the experimental conformer with that of conformer Day-1, and furthermore to over-stabilize the van Eijck-3 conformer by about 2 kJ/mol.[26]

DFT and DC-DFT results for molecule X in the gas phase are shown in Fig. 6(a). Similar to trends observed previously,[26,41] each of the GGA and meta-GGA functionals that we consider overestimates the stability of the van Eijck-3 conformer relative to the experimental one. Of the conventional (self-consistent) DFT approaches, only BLYP+D3, B3LYP+D3, and SCAN0+D3 predict qualitatively correct relative energies for the closely-spaced experimental and the Day-1 conformers, which are the least-stable conformers in isolation. On the other hand, using DC-DFT all of the functionals examined here place those two conformers in the correct energetic order. The DC procedure also reduces the overstabilization of conformer van Eijck-3, relative to the self-consistent DFT results.

Density sensitivities for conformers of molecule X are plotted in Fig. 5(b). We mainly focus on the Day-1 conformer and the experimental one since these are the relative energies that are most susceptible to switching order as one functional is swapped for another. The value of S for the Day-1 conformer is 1.7 kJ/mol larger than the value obtained for the experimental conformer, which is perhaps significant in view of the fact that these two conformers differ only by about 1 kJ/mol, according to DLPNO-CCSD(T) calculations.[26] The large sensitivity for the Day-1 conformer is consistent with its overstabilization (relative to the experimental conformer) by functionals such as PBE and PBE0. The over-stabilization of the van Eijck-3 conformer with the traditional DFT can also be explained by the larger S associated with it.

Relative polymorph energies for molecule X are given in Fig. 6(b). Once again, the predicted lattice energies improve significantly when DC-DFT is used instead of self-consistent DFT. At the same time, some of the

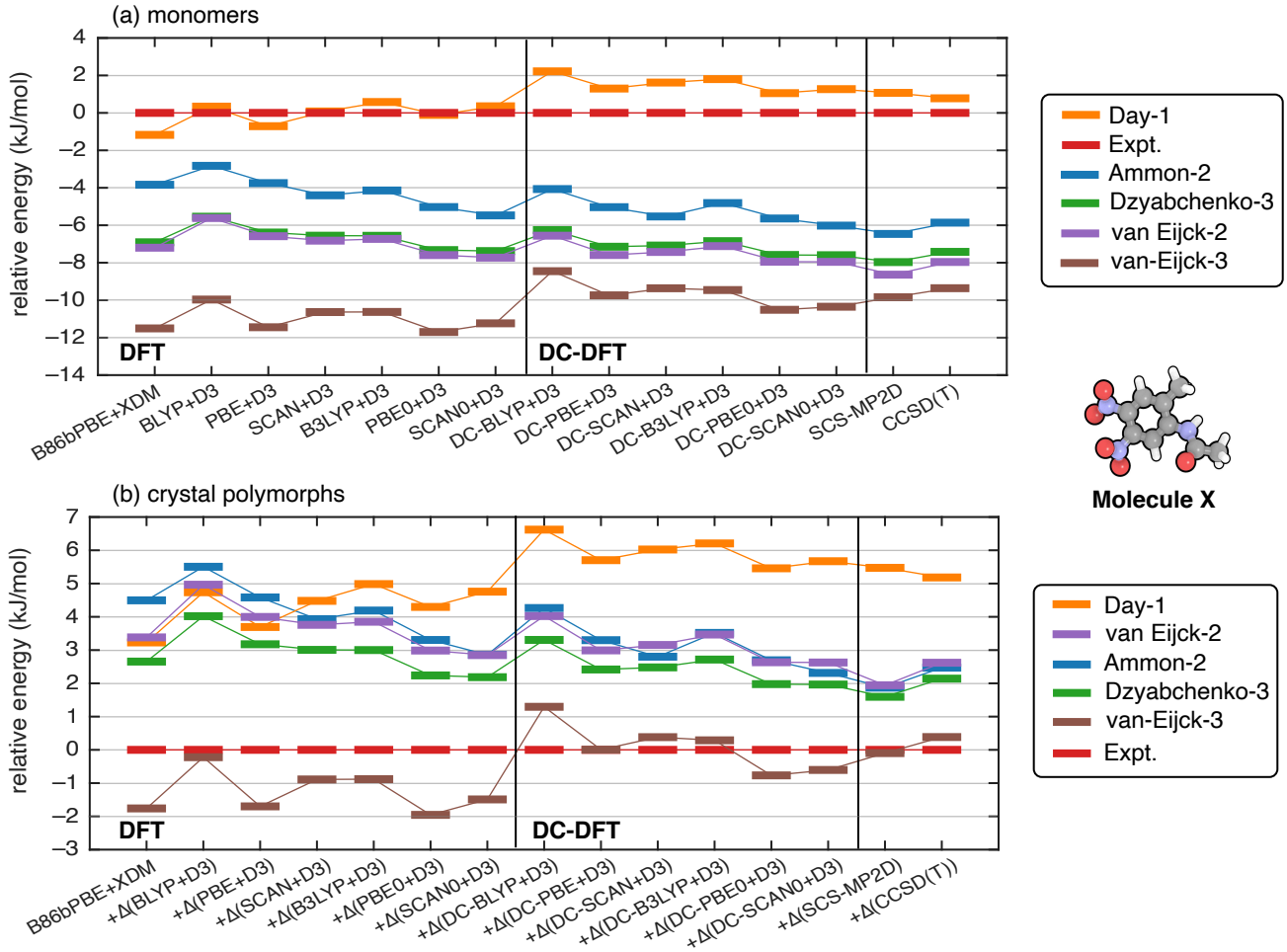

Figure 6: Energetic ordering of conformers of molecule X (Fig. 1), computed using both self-consistent DFT and DC-DFT for the same set of functionals: (a) isolated monomer energies, and (b) crystal polymorph energies, computed using the monomer-correction scheme of Eq. (8). Energies are plotted relative to "Expt.", which is the conformer found in the experimental crystal structure.

energy orderings remain sensitive to the choice of functional, even when DC-DFT is used. This largely reflects the difficulty of the problem, with relative energy changes of ~ 1 kJ/mol being enough to affect the ordering. In this particular example, DC-SCAN+D3 (based on semilocal SCAN rather than the hybrid SCAN0) best reproduces the CCSD(T) benchmarks.

We next discuss results for the anti-cancer drug axitinib. This drug has five known conformational polymorphs that are denoted I, IV, VI, XXV, and XLI, and many more multi-component crystal forms.[86,87] In most polymorphs, the axitinib molecule adopts an extended conformation but in the thermodynamically most stable XLI form, however, rotation about the sulfur group leads to a more folded conformation. In the process, the π conjugation between the aromatic ring and the terminal amide moiety is disrupted; see Fig. 1. This causes the XLI form to be artificially destabilized by GGA functionals, leading to erroneous polymorph energy rankings.[26]

Relative energies of axitinib conformers are shown in Fig. 7. New DLPNO-CCSD(T_1)/CBS calculations performed here afford the following energetic ordering for the isolated monomer:

$$\text{IVb} < \text{XLI} < \text{VI} < \text{XXV} < \text{IVa} < \text{I} \,. \qquad (11)$$

None of the self-consistent functionals reproduces this ordering, and many of the functionals (with notable exceptions BLYP+D3 and B3LYP+D3) significantly destabilize form XLI, which is the conformer that appears in the lowest-energy crystal polymorph. DC-DFT generally shifts the conformational energies in the correct direction by stabilizing XLI relative to the other conformers. However, the extent to which this is true varies by several kJ/mol depending upon the choice of functional, and for the BLYP+D3 and B3LYP+D3 functionals that perform reasonably well in conventional self-consistent calculations, the errors increase when DC-DFT is used. Other functionals do improve when DC-DFT replaces a self-consistent calculation, and the best-performing DFT approach is DC-PBE+D3, with root-mean-square (RMS)

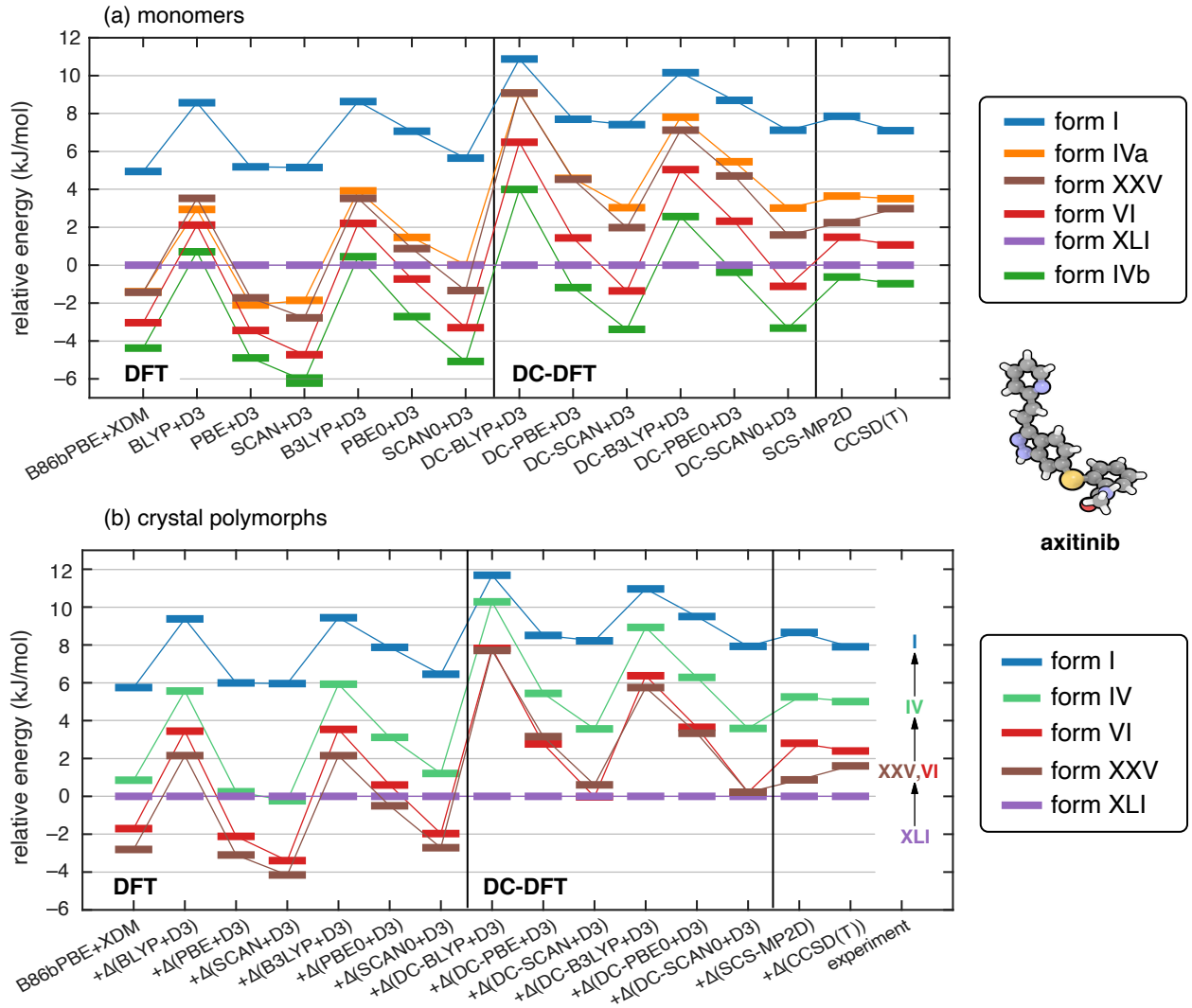

Figure 7: Energetic ordering of conformers of axitinib (Fig. 1), computed using both self-consistent DFT and DC-DFT for the same set of functionals: (a) isolated monomer energies, and (b) crystal polymorph energies, computed using the monomer-correction scheme of Eq. (8). Energies are plotted relative to that of the XLI conformer.

error of 0.9 kJ/mol with respect to the CCSD(T) benchmarks. However, SCS-MP2D does slightly better, with a RMS error of 0.5 kJ/mol.

Relative energies of the axitinib crystal polymorphs are shown in Fig. 7(b) and the various DC-DFT approaches perform similarly except that the energy gap between the lowest-energy polymorph (XLI in all cases) and the others varies by up to 8 kJ/mol depending on the choice of functional. The ordering of the (near-degenerate) polymorphs VI and XXV is uncertain in the DC-DFT calculations, but that is true experimentally as well.[88] Otherwise, DC-DFT consistently predicts the correct energetic ordering of the polymorphs, for all functionals tested, although the energies are spread out over too large a range in some cases, by up to 4 kJ/mol.

The relatively poor performance of DC-DFT for axitinib, as compared to ROY or molecule X, is a bit puzzling given that S_{atom} is smallest for axitinib. That observation, combined with the fact that self-consistent BLYP+D3 and B3LYP+D3 calculations perform well for axitinib, suggests that functional-driven error may exceed density-driven error for this molecule. Given the nature of the conformers that are considered here, the π-delocalization issues are largely confined to one end of this molecule, and the considerably larger size of axitinib (relative to either ROY or molecule X) may wash out the advantages of DC-DFT in this case. It is possible that a fragmentation approach,[89] with DC-DFT applied only to the part of the molecule that is subject to significant delocalization problems, could improve the situation, but we have not pursued such an approach here. In any case, results for axitinib highlight how density-driven error is only one factor that affects conformational energies in large, conjugated organic molecules, and caution against

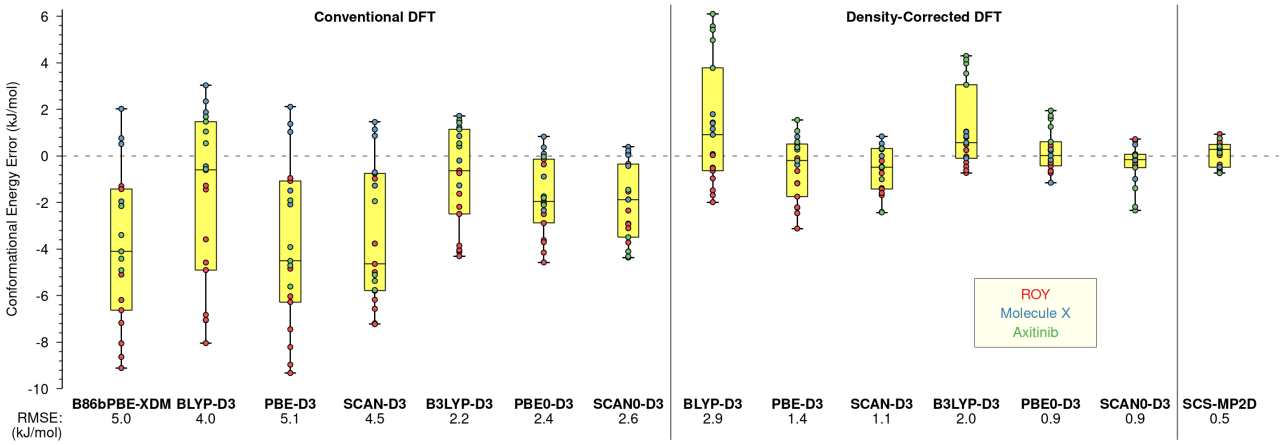

Figure 8: Summary of conformational energy errors (in kJ/mol) for isolated molecules ROY, molecule X, and axitinib, relative to CCSD(T) benchmarks. The box-and-whisker plots summarize quartiles of the error distributions, while the points show the errors for individual conformational energies.

assuming that DC-DFT is a panacea for such problems.

Stepping back from the finer details of each system, Fig. 8 plots errors in conformational energies for all three molecules (ROY, molecule X, and axitinib), relative to CCSD(T) benchmarks, indicating the RMS error for each DFT approach and for SCS-MP2D. (The RMS errors are also summarized in Fig. S3.) Relative to self-consistent DFT, the DC-DFT approach generally reduces the width of the error distributions by up to a factor of 3–4, and DC-hybrid functionals afford the tightest error distributions. At the same time, even the best of the DC-DFT models affords errors that are about twice as large as those obtained using SCS-MP2D. Taken together, these results highlight how DC-DFT models can provide a useful, pragmatic approach for improving the quality of common DFT functionals in challenging systems with density-driven delocalization error, but that higher-level methods may still be preferred for high-accuracy work.

IV. Conclusion

We have used the DC-DFT technique to study the energy landscape of several conjugated organic molecules, as well as the relative polymorph energies in the crystalline phase. These are challenging problems due to the appearance of multiple low-energy conformers (and corresponding low-energy polymorphs), and self-consistent DFT calculations with standard semilocal and hybrid functionals fail to reproduce benchmark *ab initio* results. We attribute this to SIE, in the particular form of π-delocalization error as the degree of conjugation is tuned by means of various intramolecular torsion angles. Application of DC-DFT, using the same common functionals, significantly mitigates the errors in most cases and usually results in the correction energetic ordering of crystal polymorphs, when computed by means of a monomer-correction scheme[26] applied to a periodic DFT calculation.

The DC-SCAN+D3 and DC-SCAN0+D3 methods work reasonably well for conformers and polymorphs of the benchmark ROY and molecule X systems, although the larger molecule axitinib proves to be more difficult. For axitinib, most (but not all) of the DC-DFT approaches improve upon their conventional self-consistent analogues, but none of the DFT methods produces fully satisfactory agreement with CCSD(T) benchmarks. We speculate that the relevant π-delocalization error in this case may be isolated within a particular aromatic moiety, and that DC-DFT applied to the entire (much larger) molecule may upset the balance of reasons why particular functionals perform well for the parts of the molecule that do not suffer from over-delocalization of π electrons. A fragmentation strategy might help, with DC-DFT applied only to part of the molecule, but in any case this system highlights potential difficulties in applying DC-DFT to systems where SIE problems are confined to a relatively small portion of a much larger molecule. Overall, our results underscore previous work[26,40] indicating that monomer-corrected periodic GGA calculations, with an appropriately selected level of theory for the monomer corrections, is an effective and low-cost strategy for polymorphic molecular crystals.

Acknowledgements

Work by B.R. and J.M.H. was supported by National Science Foundation grant no. CHE-1955282, with calculations performed at the Ohio Supercomputer Center.[90] G.J.O.B. acknowledges support from the National Science Foundation (CHE-1955554) and supercomputer

time from XSEDE (TG-CHE110064). The authors express condolences for the family of Prof. Nick Besley, who was a valued member of the Q-Chem community.

Disclosure statement

J.M.H. serves on the board of directors of Q-Chem Inc.

References

[1] D. Braga, F. Grepioni, L. Maini, and M. Polito, "Crystal polymorphism and multiple crystal forms", in *Molecular Networks*, M. W. Hosseini, Ed., Vol. 132 of *Structure and Bonding;* Springer-Verlag: Berlin, 2009; pages 25–50.

[2] A. J. Cruz-Cabeza and J. Bernstein, "Conformational polymorphism", *Chem. Rev.*, **114**, 2170–2191 (2014).

[3] Y. Zhou, J. Wang, Y. Xiao, T. Wang, and X. Huang, "The effects of polymorphism on physicochemical properties and pharmacodynamics of solid drugs", *Curr. Pharm. Design*, **24**, 2375–2382 (2018).

[4] A. J. Cruz-Cabeza, S. M. Reutzel-Edens, and J. Bernstein, "Facts and fictions about polymorphism", *Chem. Soc. Rev.*, **44**, 8619–8635 (2015).

[5] J. Nyman and S. M. Reutzel-Edens, "Crystal structure prediction is changing from basic science to applied technology", *Faraday Discuss.*, **211**, 459–476 (2018).

[6] J. Bauer, S. Spanton, R. Henry, J. Quick, W. Dziki, W. Porter, and J. Morris, "Ritonavir: An extraordinary example of conformational polymorphism", *Pharm. Res.*, **18**, 859–866 (2001).

[7] I. B. Rietveld and R. Ceolin, "Rotigotine: Unexpected polymorphism with predictable overall monotropic behavior", *J. Pharm. Sci.*, **104**, 4117–4122 (2015).

[8] J. D. Dunitz and J. Bernstein, "Disappearing polymorphs", *Acc. Chem. Res.*, **28**, 193–200 (1995).

[9] D. Bučar, R. W. Lancaster, and J. Bernstein, "Disappearing polymorphs revisited", *Angew. Chem. Int. Ed. Engl.*, **54**, 6972–6993 (2015).

[10] M. A. Neumann and J. van de Streek, "How many ritonavir cases are there still out there?", *Faraday Discuss.*, **211**, 441–458 (2018).

[11] J. Maddox, "Crystals from first principles", *Nature*, **335**, 201 (1988).

[12] A. Gavezzotti, "Are crystal structures predictable?", *Acc. Chem. Res.*, **27**, 309–314 (1994).

[13] G. M. Day, T. G. Cooper, A. J. Cruz-Cabeza, K. E. Hejczyk, H. L. Ammon, S. X. M. Boerrigter, J. S. Tan, R. G. Della Valle, E. Venuti, J. Jose, S. R. Gadre, G. R. Desiraju, T. S. Thakur, B. P. van Eijck, J. C. Facelli, V. E. Bazterra, M. B. Ferraro, D. W. M. Hoffman, M. A. Neumann, F. J. J. Leusen, J. Kendrick, S. L. Price, A. J. Misquitta, P. G. Karamertzanis, G. W. A. Welch, H. A. Scheraga, Y. A. Arnautova, M. U. Schmidt, J. van de Streek, A. K. Wolf, and B. Schweizer, "Significant progress in predicting the crystal structures of small organic molecules—a report on the fourth blind test", *Acta Cryst. B*, **65**, 107–125 (2009).

[14] D. A. Bardwell, C. S. Adjiman, Y. A. Arnautova, E. Bartashevich, S. X. M. Boerrigter, D. E. Braun, A. J. Cruz-Cabeza, G. M. Day, R. G. Della Valle, G. R. Desiraju, B. P. van Eijck, J. C. Facelli, M. B. Ferraro, D. Grillo, M. Habgood, D. W. M. Hofmann, F. Hofmann, K. V. J. Jose, P. G. Karamertzanis, A. V. Kazantsev, J. Kendrick, L. N. Kuleshova, F. J. J. Leusen, A. V. Maleev, A. J. Misquitta, S. Mohamed, R. J. Needs, M. A. Neumann, D. Nikylov, A. M. Orendt, R. Pal, C. C. Pantelides, C. J. Pickard, L. S. Price, S. L. Price, H. A. Scheraga, J. van de Streek, T. S. Thakur, S. Tiwari, E. Venuti, and I. K. Zhitkov, "Towards crystal structure prediction of complex organic compounds—a report on the fifth blind test", *Acta Cryst. B*, **67**, 535–551 (2011).

[15] A. M. Reilly, R. I. Cooper, C. S. Adjiman, S. Bhattacharya, A. D. Boese, J. G. Brandenburg, P. J. Bygrave, R. Bylsma, J. E. Campbell, R. Car, D. H. Case, R. Chadha, J. C. Cole, K. Cosburn, H. M. Cuppen, F. Curtis, G. M. Day, R. A. DiStasio Jr., A. Dzyabchenko, B. P. van Eijck, D. M. Elking, J. A. van den Ende, J. C. Facelli, M. B. Ferraro, L. Fusti-Molnar, C.-A. Gatsiou, T. S. Gee, R. de Gelder, L. M. Ghiringhelli, H. Goto, S. Grimme, R. Guo, D. W. M. Hofmann, J. Hoja, R. K. Hylton, L. Iuzzolino, W. Jankiewicz, D. T. de Jong, J. Kendrick, N. J. J. de Klerk, H.-Y. Ko, L. N. Kuleshova, X. Li, S. Lohani, F. J. J. Leusen, A. M. Lund, J. Lv, Y. Ma, N. Marom, A. E. Masunov, P. McCabe, D. P. McMahon, H. Meekes, M. P. Metz, A. J. Misquitta, S. Mohamed, B. Monserrat, R. J. Needs, M. A. Neumann, J. Nyman, S. Obata, H. Oberhofer, A. R. Oganov, A. M. Orendt, G. I. Pagola, C. C. Pantelides, C. J. Pickard, R. Podeszwa, L. S. Price, S. L. Price, A. Pulido, M. G. Read, K. Reuter, E. Schneider, C. Schober, G. P. Shields, P. Singh, I. J. Sugden, K. Szalewicz, C. R. Taylor, A. Tkatchenko, M. E. Tuckerman, F. Vaccaro, M. Vasileiadis, A. Vazquez-Mayagoitia, L. Vogt, Y. Wang, R. E. Watson, G. A. de Wiijs, J. Yang, Q. Zhu, and C. R. Groom, "Report on the sixth blind test of organic crystal structure prediction methods", *Acta Cryst. B*, **72**, 439–459 (2016).

[16] A. Otero-de-la-Roza, B. H. Cao, I. K. Price, J. E. Hein, and E. R. Johnson, "Predicting relative solubilities of racemic and enantiopure crystals by density functional theory", *Angew. Chem. Int. Ed. Engl.*, **53**, 7879–7882 (2014).

[17] G. J. O. Beran, "A new era for ab initio molecular crystal lattice energy prediction", *Angew. Chem. Int. Ed. Engl.*, **54**, 396–398 (2015).

[18] G. J. O. Beran, "Modeling polymorphic molecular crystals with electronic structure theory", *Chem. Rev.*, **116**, 5567–5613 (2016).

[19] E. Zurek, "Discovering new materials via *a priori* crystal structure prediction", in *Reviews in Computational Chemistry*, A. L. Parrill and K. B. Lipkowitz, Eds., Vol. 29; Wiley-VCH: Hoboken, NJ, 2016; pages 274–326.

[20] S. L. Price and J. G. Brandenburg, "Molecular crystal structure prediction", in *Non-Covalent Interactions in Quantum Chemistry and Physics*, A. O. de la Roza and G. A. DiLabio, Eds.; Elsevier: Amsterdam, 2017; chapter 11, pages 333–363.

[21] A. Pulido, L. Chen, T. Kaczorowski, D. Holden, M. A. Little, S. Y. Chong, B. J. Slater, D. P. McMahon, B. Bonillo, C. J. Stackhouse, A. Stephenson, C. M. Kane, R. Clowes, T. Hasell, A. I. Cooper, and G. M. Day, "Functional materials discovery using energy–structure–function maps", *Nature*, **543**, 657–664 (2017).

[22] J. Hoja, H.-Y. Ko, M. A. Neumann, R. Car, R. A. DiStasio Jr., and A. Tkatchenko, "Reliable and practical computational description of molecular crystal polymorphs", *Sci.*

Adv., **5**, eaau3338:1–10 (2019).

[23] G. Sun, X. Liu, Y. A. Abramov, S. O. N. Lill, C. Chang, V. Burger, and A. Broo, "Current state-of-the-art in-house and cloud-based applications of virtual polymorph screening of pharmaceutical compounds: A challenging case of AZD1305", *Crys. Growth Des.*, **21**, 1872–1983 (2021).

[24] Y. N. Heit, K. D. Nanda, and G. J. O. Beran, "Predicting finite-temperature properties of crystalline carbon dioxide from first principles with quantitative accuracy", *Chem. Sci.*, **7**, 246–255 (2016).

[25] C. Červinka and G. J. O. Beran, "*Ab initio* prediction of the polymorph phase diagram for crystalline methanol", *Chem. Sci.*, **9**, 4622–4629 (2018).

[26] C. Greenwell and G. J. O. Beran, "Inaccurate conformational energies still hinder crystal structure prediction in flexible organic molecules", *Crys. Growth Des.*, **20**, 4875–4881 (2020).

[27] J. Nyman and G. M. Day, "Static and lattice vibrational energy differences between polymorphs", *CrystEngComm*, **17**, 5154–5165 (2015).

[28] C. Greenwell, J. L. McKinley, P. Zhang, Q. Zeng, G. Sun, B. Li, S. Wen, and G. J. O. Beran, "Overcoming the difficulties of predicting conformational polymorph energetics in molecular crystals *via* correlated wavefunction methods", *Chem. Sci.*, **11**, 2200–2214 (2020).

[29] P. G. Karamertzanis, G. M. Day, G. W. A. Welch, J. Kendrick, F. J. J. Leusen, M. A. Neumann, and S. L. Price, "Modeling the interplay of inter-and intramolecular hydrogen bonding in conformational polymorphs", *J. Chem. Phys.*, **128**, 244708:1–17 (2008).

[30] M. A. Neumann, F. J. J. Leusen, and J. Kendrick, "A major advance in crystal structure prediction", *Angew. Chem. Int. Ed. Engl.*, **120**, 2461–2464 (2008).

[31] J. Kendrick, M. D. Gourlay, M. A. Neumann, and F. J. J. Leusen, "Predicting spontaneous racemate resolution using recent developments in crystal structure prediction", *CrystEngComm*, **11**, 2391–2399 (2009).

[32] A. M. Reilly and A. Tkatchenko, "Role of dispersion interactions in the polymorphism and entropic stabilization of the aspirin crystal", *Phys. Rev. Lett.*, **113**, 055701:1–5 (2014).

[33] F. Curtis, X. Li, T. Rose, A. Vásquez-Mayagoitia, S. Bhattacharya, L. M. Ghiringhelli, and N. Marom, "GAtor: A first-principles genetic algorithm for molecular crystal structure prediction", *J. Chem. Theory Comput.*, **14**, 2246–2264 (2018).

[34] I. Bier, D. O'Connor, Y.-T. Hsieh, W. Wen, A. M. Hiszpanski, T. Y.-J. Han, and N. Marom, "Crystal structure prediction of energetic materials and a twisted arene with Genarris and GAtor", *CrystEngComm*, **23**, 6023–6038 (2021).

[35] J. Nyman, L. Yu, and S. M. Reutzel-Edens, "Accuracy and reproducibility in crystal structure prediction: The curious case of ROY", *CrystEngComm*, **21**, 2080–2088 (2019).

[36] G. J. O. Beran, S. E. Wright, C. Greenwell, and A. J. Cruz-Cabeza, "The interplay of intra- and intermolecular errors in modeling conformational polymorphs", *J. Chem. Phys.*, **156**, 104112:1–16 (2022).

[37] A. J. Cohen, P. Mori-Sanchez, and W. Yang, "Challenges for density functional theory", *Chem. Rev.*, **112**, 289–320 (2012).

[38] C. Greenwell and G. J. O. Beran, "Rubrene untwisted: Common density functional theory calculations overestimate its deviant tendencies", *J. Mater. Chem. C*, **9**, 2848–2857 (2021).

[39] M. Tan, A. G. Shtukenberg, S. Zhu, W. Xu, E. Dooryhee, S. M. Nichols, M. D. Ward, B. Kahr, and Q. Zhu, "ROY revisited, again: The eighth solved structure", *Faraday Discuss.*, **211**, 477–491 (2018).

[40] G. J. O. Beran, I. J. Sugden, C. Greenwell, D. H. Bowskill, C. C. Pantelides, and C. S. Adjiman, "How many more polymorphs of ROY remain undiscovered?", *Chem. Sci.*, **13**, 1288–1297 (2022).

[41] S. R. Whittleton, A. Otero-de-la-Roza, and E. R. Johnson, "Exchange-hole dipole dispersion model for accurate energy ranking in molecular crystal structure prediction II: Nonplanar molecules", *J. Chem. Theory Comput.*, **13**, 5332–5342 (2017).

[42] G. M. Day, W. D. S. Motherwell, H. L. Ammon, S. X. M. Boerrigter, R. G. Della Valle, E. Venuti, A. Dzyabchenko, J. D. Dunitz, B. Scweizer, B. P. avn Eijck, P. Erk, J. C. Facelli, V. E. Bazterra, M. B. Ferraro, D. W. M. Hofmann, F. J. J. Leusen, C. Liang, C. C. Pantelides, P. G. Karamertzanis, S. L. Price, T. C. Lewis, H. Nowell, A. Torrisi, H. A. Scheraga, Y. A. Arnautova, M. U. Schmidt, and P. Verwer, "A third blind test of crystal structure prediction", *Acta Cryst. B*, **61**, 511–527 (2005).

[43] T. J. Gately, W. Sontising, C. J. Easley, I. Islam, R. O. Al-Kaysi, G. J. O. Beran, and C. J. Bardeen, "Effect of halogen substitution on energies and dynamics of reversible photomechanical crystals based on 9-anthracenecarboxylic acid", *CrystEngComm*, **23**, 5931–5943 (2021).

[44] A. D. Becke, "On the large-gradient behavior of the density functional exchange energy", *J. Chem. Phys.*, **85**, 7184–7187 (1986).

[45] J. P. Perdew, K. Burke, and M. Ernzerhof, "Generalized gradient approximations made simple", *Phys. Rev. Lett.*, **77**, 3865–3868 (1996). Erratum: *ibid.* **78**, 1396 (1997).

[46] A. Otero-de-la-Roza and E. R. Johnson, "Van der Waals interactions in solids using the exchange-hole dipole moment model", *J. Chem. Phys.*, **136**, 174109:1–8 (2012).

[47] J. Řezác, C. Greenwell, and G. J. O. Beran, "Accurate noncovalent interactions via dispersion-corrected second-order Møller–Plesset perturbation theory", *J. Chem. Theory Comput.*, **14**, 4711–4721 (2018).

[48] C. Greenwell, J. Řezáč, and G. J. O. Beran, "Spin-component-scaled and dispersion-corrected second-order Møller–Plesset perturbation theory: A path toward chemical accuracy", *Phys. Chem. Chem. Phys.*, **24**, 3695–3712 (2021).

[49] M.-C. Kim, E. Sim, and K. Burke, "Understanding and reducing errors in density functional calculations", *Phys. Rev. Lett.*, **111**, 073003:1–5 (2013).

[50] M.-C. Kim, E. Sim, and K. Burke, "Ions in solution: Density corrected density functional theory (DC-DFT)", *J. Chem. Phys.*, **140**, 18A528:1–10 (2014).

[51] M.-C. Kim, H. Park, S. Son, E. Sim, and K. Burke, "Improved DFT potential energy surfaces via improved densities", *J. Phys. Chem. Lett.*, **6**, 3802–3807 (2015).

[52] S. Vuckovic, S. Song, J. Kozlowski, E. Sim, and K. Burke, "Density functional analysis: The theory of density-corrected DFT", *J. Chem. Theory Comput.*, **15**, 6336–6346 (2019).

[53] E. Sim, S. Song, and K. Burke, "Quantifying density errors in DFT", *J. Phys. Chem. Lett.*, **9**, 6385–6392 (2018).

[54] S. Song, S. Vuckovic, E. Sim, and K. Burke, "Density sensitivity of empirical functionals", *J. Phys. Chem. Lett.*, **12**, 800–807 (2021).

[55] S. Song, S. Vuckovic, E. Sim, and K. Burke, "Density-corrected DFT explained: Questions and answers", *J. Chem. Theory Comput.*, **18**, 817–827 (2022).

[56] N. Oliphant and R. Bartlett, "A systematic comparison of molecular properties obtained using Hartree–Fock, a hybrid Hartree–Fock density-functional-theory, and coupled-cluster methods", *J. Chem. Phys.*, **100**, 6550–6561 (1994).

[57] P. Verma, A. Perera, and R. J. Bartlett, "Increasing the applicability of DFT I: Non-variational correlation corrections from Hartree–Fock DFT for predicting transition states", *Chem. Phys. Lett.*, **524**, 10–15 (2012).

[58] B. G. Janesko and G. E. Scuseria, "Hartree–Fock orbitals significantly improve the reaction barrier heights predicted by semilocal density functionals", *J. Chem. Phys.*, **128**, 244112:1–4 (2008).

[59] B. Rana, M. P. Coons, and J. M. Herbert, "Detection and correction of delocalization errors for electron and hole polarons using density-corrected DFT", *J. Phys. Chem. Lett.*, **13**, 5275–5284 (2022).

[60] S. Nam, E. Cho, E. Sim, and K. Burke, "Explaining and fixing DFT failures for torsional barriers", *J. Phys. Chem. Lett.*, **12**, 2796–2804 (2021).

[61] Y. Kim, S. Song, E. Sim, and K. Burke, "Halogen and chalcogen binding dominated by density-driven errors", *J. Phys. Chem. Lett.*, **10**, 295–301 (2019). Erratum: *ibid.* **11**, 8041 (2020).

[62] G. Santra and J. M. L. Martin, "What types of chemical problems benefit from density-corrected DFT? A probe using an extensive and chemically diverse test suite", *J. Chem. Theory Comput.*, **17**, 1368–1379 (2021).

[63] Y. Zhang and W. Yang, "A challenge for density functionals: Self-interaction error increases for systems with a noninteger number of electrons", *J. Chem. Phys.*, **109**, 2604–2608 (1998).

[64] A. Ruzsinszky, J. P. Perdew, G. I. Csonka, O. A. Vydrov, and G. E. Scuseria, "Spurious fractional charge of dissociated atoms: Pervasive and resilient self-interaction error of common density functionals", *J. Chem. Phys.*, **125**, 194112:1–8 (2006).

[65] E. Epifanovsky, A. T. B. Gilbert, X. Feng, J. Lee, Y. Mao, N. Mardirossian, P. Pokhilko, A. F. White, M. P. Coons, A. L. Dempwolff, Z. Gan, D. Hait, P. R. Horn, L. D. Jacobson, I. Kaliman, J. Kussmann, A. W. Lange, K. U. Lao, D. S. Levine, J. Liu, S. C. McKenzie, A. F. Morrison, K. D. Nanda, F. Plasser, D. R. Rehn, M. L. Vidal, Z.-Q. You, Y. Zhu, B. Alam, B. J. Albrecht, A. Aldossary, E. Alguire, J. H. Andersen, V. Athavale, D. Barton, K. Begam, A. Behn, N. Bellonzi, Y. A. Bernard, E. J. Berquist, H. G. A. Burton, A. Carreras, K. Carter-Fenk, R. Chakraborty, A. D. Chien, K. D. Closser, V. Cofer-Shabica, S. Dasgupta, M. de Wergifosse, J. Deng, M. Diedenhofen, H. Do, S. Ehlert, P.-T. Fang, S. Fatehi, Q. Feng, T. Friedhoff, J. Gayvert, Q. Ge, G. Gidofalvi, M. Goldey, J. Gomes, C. E. González-Espinoza, S. Gulania, A. O. Gunina, M. W. D. Hanson-Heine, P. H. P. Harbach, A. Hauser, M. F. Herbst, M. Hernández Vera, M. Hodecker, Z. C. Holden, S. Houck, X. Huang, K. Hui, B. C. Huynh, M. Ivanov, A. Jász, H. Ji, H. Jiang, B. Kaduk, S. Kähler, K. Khistyaev, J. Kim, G. Kis, P. Klunzinger, Z. Koczor-Benda, J. H. Koh, D. Kosenkov, L. Koulias, T. Kowalczyk, C. M. Krauter, K. Kue, A. Kunitsa, T. Kus, I. Ladjánszki, A. Landau, K. V. Lawler, D. Lefrancois, S. Lehtola, R. R. Li, Y.-P. Li, J. Liang, M. Liebenthal, H.-H. Lin, Y.-S. Lin, F. Liu, K.-Y. Liu, M. Loipersberger, A. Luenser, A. Manjanath, P. Manohar, E. Mansoor, S. F. Manzer, S.-P. Mao, A. V. Marenich, T. Markovich, S. Mason, S. A. Maurer, P. F. McLaughlin, M. F. S. J. Menger, J.-M. Mewes, S. A. Mewes, P. Morgante, J. W. Mullinax, K. J. Oosterbaan, G. Paran, A. C. Paul, S. K. Paul, F. Pavošević, Z. Pei, S. Prager, E. I. Proynov, A. Rák, E. Ramos-Cordoba, B. Rana, A. E. Rask, A. Rettig, R. M. Richard, F. Rob, E. Rossomme, T. Scheele, M. Scheurer, M. Schneider, N. Sergueev, S. M. Sharada, W. Skomorowski, D. W. Small, C. J. Stein, Y.-C. Su, E. J. Sundstrom, Z. Tao, J. Thirman, G. J. Tornai, T. Tsuchimochi, N. M. Tubman, S. P. Veccham, O. Vydrov, J. Wenzel, J. Witte, A. Yamada, K. Yao, S. Yeganeh, S. R. Yost, A. Zech, I. Y. Zhang, X. Zhang, Y. Zhang, D. Zuev, A. Aspuru-Guzik, A. T. Bell, N. A. Besley, K. B. Bravaya, B. R. Brooks, D. Casanova, J.-D. Chai, S. Coriani, C. J. Cramer, G. Cserey, A. E. DePrince III, R. A. DiStasio Jr., A. Dreuw, B. D. Dunietz, T. R. Furlani, W. A. Goddard III, S. Hammes-Schiffer, T. Head-Gordon, W. J. Hehre, C.-P. Hsu, T.-C. Jagau, Y. Jung, A. Klamt, J. Kong, D. S. Lambrecht, W. Liang, N. J. Mayhall, C. W. McCurdy, J. B. Neaton, C. Ochsenfeld, J. A. Parkhill, R. Peverati, V. A. Rassolov, Y. Shao, L. V. Slipchenko, T. Stauch, R. P. Steele, J. E. Subotnik, A. J. W. Thom, A. Tkatchenko, D. G. Truhlar, T. Van Voorhis, T. A. Wesolowski, K. B. Whaley, H. L. Woodcock III, P. M. Zimmerman, S. Faraji, P. M. W. Gill, M. Head-Gordon, J. M. Herbert, and A. I. Krylov, "Software for the frontiers of quantum chemistry: An overview of developments in the Q-Chem 5 package", *J. Chem. Phys.*, **155**, 084801:1–59 (2021).

[66] S. Dasgupta and J. M. Herbert, "Standard grids for high-precision integration of modern density functionals: SG-2 and SG-3", *J. Comput. Chem.*, **38**, 869–882 (2017).

[67] S. Grimme, J. Antony, S. Ehrlich, and H. Krieg, "A consistent and accurate *ab initio* parameterization of density functional dispersion correction (DFT-D) for the 94 elements H–Pu", *J. Chem. Phys.*, **132**, 154104:1–19 (2010).

[68] J. Sun, A. Ruzsinszky, and J. P. Perdew, "Strongly constrained and appropriately normed semilocal density functional", *Phys. Rev. Lett.*, **115**, 036402:1–6 (2015).

[69] A. Szabo and N. S. Ostlund, "The correlation energy in the random phase approximation: Intermolecular forces between closed-shell systems", *J. Chem. Phys.*, **67**, 4351–4360 (1977).

[70] R. Bukowski, R. Podeszwa, and K. Szalewicz, "Efficient calculation of coupled Kohn–Sham dynamic susceptibility functions and dispersion energies with density fitting", *Chem. Phys. Lett.*, **414**, 111–116 (2005).

[71] A. Heßelmann, "Improved supermolecular second order Møller–Plesset intermolecular interaction energies using time-dependent density functional response theory", *J. Chem. Phys.*, **128**, 144112:1–9 (2008).

[72] Y. Guo, C. Riplinger, U. Becker, D. G. Liakos, Y. Minenkov, L. Cavallo, and F. Neese, "Communication: An improved linear scaling perturbative triples correction for the domain based local pair-natural orbital based singles and doubles coupled cluster method [DLPNO-CCSD(T)]", *J. Chem. Phys.*, **148**, 011101:1–5 (2018).

[73] F. Neese, F. Wennmohs, U. Becker, and C. Riplinger, "The ORCA quantum chemistry program package", *J. Chem. Phys.*, **152**, 224108:1–18 (2020).

[74] A. Bajaj, J. P. Janet, and H. J. Kulik, "Communication: Recovering the flat-plane condition in electronic structure

theory at semi-local DFT cost", *J. Chem. Phys.*, **147**, 191101:1–5 (2017).

[75] S. Hirata, M. Head-Gordon, and R. J. Bartlett, "Configuration interaction singles, time-dependent Hartree–Fock, and time-dependent density functional theory for the electronic excited states of extended systems", *J. Chem. Phys.*, **111**, 10774–10786 (1999).

[76] K. I. Igumenshchev, S. Tretiak, and V. Y. Chernyak, "Excitonic effects in a time-dependent density functional theory", *J. Chem. Phys.*, **127**, 114902:1–9 (2007).

[77] S. A. Mewes, F. Plasser, and A. Dreuw, "Universal exciton size in organic polymers is determined by nonlocal orbital exchange in time-dependent density functional theory", *J. Phys. Chem. Lett.*, **8**, 1205–1210 (2017).

[78] L. Yu, "Polymorphism in molecular crystals: An extraordinary system of red, orange, and yellow crystals", *Acc. Chem. Res.*, **43**, 1257–1266 (2010).

[79] S. P. Thomas and M. A. Spackman, "The polymorphs of ROY: A computational study of lattice energies and conformational energy differences", *Aust. J. Chem.*, **71**, 279–284 (2018).

[80] X. Feng, A. D. Becke, and E. R. Johnson, "Theoretical investigation of polymorph- and coformer-dependent photoluminescence in molecular crystals", *CrystEngComm*, **23**, 4264–4271 (2021).

[81] W. A. Ogden, S. Ghosh, M. J. Bruzek, K. A. McGarry, L. Balhorn, V. Young, Jr., L. J. Purvis, S. E. Wegwerth, Z. Zhang, N. A. Serratore, C. J. Cramer, L. Gagliardi, and C. J. Douglas, "Partial fluorination as a strategy for crystal engineering of rubrene derivatives", *Crys. Growth Des.*, **17**, 643–658 (2017).

[82] Z. Zhang, W. A. Ogden, V. G. Young Jr., and C. J. Douglas, "Synthesis, electrochemical properties, and crystal packing of perfluororubrene", *ChemComm*, **52**, 8127–8130 (2016).

[83] Y. Sakamoto and T. Suzuki, "Perfluorinated and half-fluorinated rubrenes: Synthesis and crystal packing arrangements", *J. Org. Chem*, **82**, 8111–8116 (2017).

[84] F. Anger, T. Breuer, A. Ruff, M. Klues, A. Gerlach, R. Scholz, S. Ludwigs, G. Witte, and F. Schreiber, "Enhanced stability of rubrene against oxidation by partial and complete fluorination", *J. Phys. Chem. C*, **120**, 5515–5522 (2016).

[85] S. Dasgupta, E. Lambros, J. P. Perdew, and F. Paesani, "Elevating density functional theory to chemical accuracy for water simulations through a density-corrected many-body formalism", *Nat. Commun.*, **12**, 6359:1–12 (2021).

[86] B. P. Chekal, A. M. Campeta, Y. A. Abramov, N. Feeder, P. P. Glynn, R. W. McLaughlin, P. A. Meenan, and R. A. Singer, "The challenges of developing an API crystallization process for a complex polymorphic and highly solvated system. Part I", *Org. Process Res. Dev.*, **13**, 1327–1337 (2009).

[87] A. M. Campeta, B. P. Chekal, Y. A. Abramov, P. A. Meenan, M. J. Henson, B. Shi, R. A. Singer, and K. R. Horspool, "Development of a targeted polymorph screening approach for a complex polymorphic and highly solvating API", *J. Pharm. Sci.*, **99**, 3874–3886 (2010).

[88] M. Vasileiadis, C. C. Pantelides, and C. S. Adjiman, "Prediction of the crystal structures of axitinib, a polymorphic pharmaceutical molecule", *Chem. Eng. Sci.*, **121**, 60–76 (2015).

[89] J. M. Herbert, "Fantasy versus reality in fragment-based quantum chemistry", *J. Chem. Phys.*, **151**, 170901:1–38 (2019).

[90] Ohio Supercomputer Center, http://osc.edu/ark:/19495/f5s1ph73.